

U.S. DEPARTMENT OF COMMERCE
NATIONAL OCEANIC AND ATMOSPHERIC ADMINISTRATION
NATIONAL WEATHER SERVICE
NATIONAL METEOROLOGICAL CENTER

OFFICE NOTE 222

A Note on Tuning the Gradient Wind Relation
Currently Used in the LFM

Edward A. O'Lenic
Development Division

AUGUST 1980

This is an unreviewed manuscript, primarily
intended for informal exchange of information
among NMC staff members.

Introduction

An effort to choose a wind relation to calculate winds from heights for use in the Optimum Interpolation system (O/I) in regions of sparse wind observations, has prompted the evaluation of various wind relations during the past year. The simplest wind relation to incorporate curvature effects is the gradient wind equation, a modified version of which is now used in the analysis portion of the LFM (Brown, 1971).

Background

The gradient wind relation under investigation may be derived from the invariant form of the equations of motion in component form, in pressure coordinates,

$$\begin{aligned} \frac{\partial u}{\partial t_p} + \frac{\partial}{\partial x} \left(\phi + \frac{u^2 + v^2}{2} \right) - (\zeta + f)v + \frac{\omega \partial u}{\partial p} &= 0 \\ \frac{\partial v}{\partial t_p} + \frac{\partial}{\partial y} \left(\phi + \frac{u^2 + v^2}{2} \right) + (\zeta + f)u + \frac{\omega \partial v}{\partial p} &= 0 \end{aligned} \quad (1)$$

where

$$\phi = gZ$$

$$g = 9.8 \text{ ms}^{-2}$$

Z = height of pressure surface

u = eastward component of wind

v = northward component of wind

ζ = relative vorticity of wind

$$= \frac{\partial v}{\partial x} - \frac{\partial u}{\partial y}$$

f = coriolis parameter

$$\omega = dp/dt$$

Assuming ω -terms are negligible and letting $\partial \phi / \partial x = fv_g$, and $\partial \phi / \partial y = -fu_g$, where u_g and v_g are the geostrophic wind components,

and $K = \frac{u^2 + v^2}{2}$, we get

$$\begin{aligned} \frac{\partial u}{\partial t} + fv_g + \left(\frac{\partial K}{\partial x} - v\zeta \right) - fv &= 0 \\ \frac{\partial v}{\partial t} - fu_g + \left(\frac{\partial K}{\partial y} + u\zeta \right) + fu &= 0 \end{aligned} \quad (2)$$

Assuming that the horizontal accelerations, $\frac{\partial u}{\partial t}$, $\frac{\partial v}{\partial t}$, may be absorbed into a constant factor, k_1 , applied to the non-linear term, and further, that vorticity and kinetic energy may be approximated by their geostrophic counterparts, we get

$$u^* = u_g - \frac{k_1 k_2}{f} \left(\frac{\partial K_g}{\partial y} + u_g \zeta_g \right)$$

$$v^* = v_g + \frac{k_1 k_2}{f} \left(\frac{\partial K_g}{\partial x} - v_g \zeta_g \right)$$
(3)

where u^* , v^* = gradient wind components,

$$k_2 = \frac{\sin L - \sin 20}{\sin 30 - \sin 20}, \quad 0 \leq k_2 \leq 1 \text{ for } 20^\circ \leq L \leq 30^\circ.$$

k_2 is a latitude weighting parameter which has been inserted in equations (3) to facilitate a gradual transition from gradient winds northward of 30°N , where $k_2 = 1$, to geostrophic winds south of 20°N , where $k_2 = 0$. The parameter k_1 , is the subject of the efforts described in the next sections. In vector form, equations (3) become

$$\mathbf{w}^* = \mathbf{w}_g + \frac{k_1 k_2}{f} (\mathbf{k} \times \nabla K_g - \mathbf{w}_g \zeta_g)$$
(4)

Procedure

Seven synoptic cases* were chosen from which to compute gradient winds (Appendix A). For each case, 10 sets of winds, each using a different value of k_1 , were calculated and verified against observations using the SUMAC verification code. Verification statistics were compiled for the 110 station NA110 area and the 96 station EUR96 area (Figure 1).

Results

Graphs of RMS vector wind deviation and bias (gradient versus observed) versus k_1 (Appendix B) show that, while the RMS generally reached a minimum for $0.10 \leq k_1 \leq 0.25$, the gradient winds exhibited a negative bias which decreases monotonically with increasing k_1 . Further, this bias has its largest magnitude and most rapid rate of decrease at 250 mb, where it varies from about -1 ms^{-1} to -3 ms^{-1} for $0.05 \leq k_1 \leq 0.33$. This behavior of the bias indicates that the non-linear term, $\mathbf{k} \times \nabla K_g - \mathbf{w}_g \zeta_g$,

was negative below 100 mb for all values of k_1 for all 7 cases in the test. Thus, the effects of cyclonic curvature apparently dominated the

* NOTE: Hough height analyses were used.

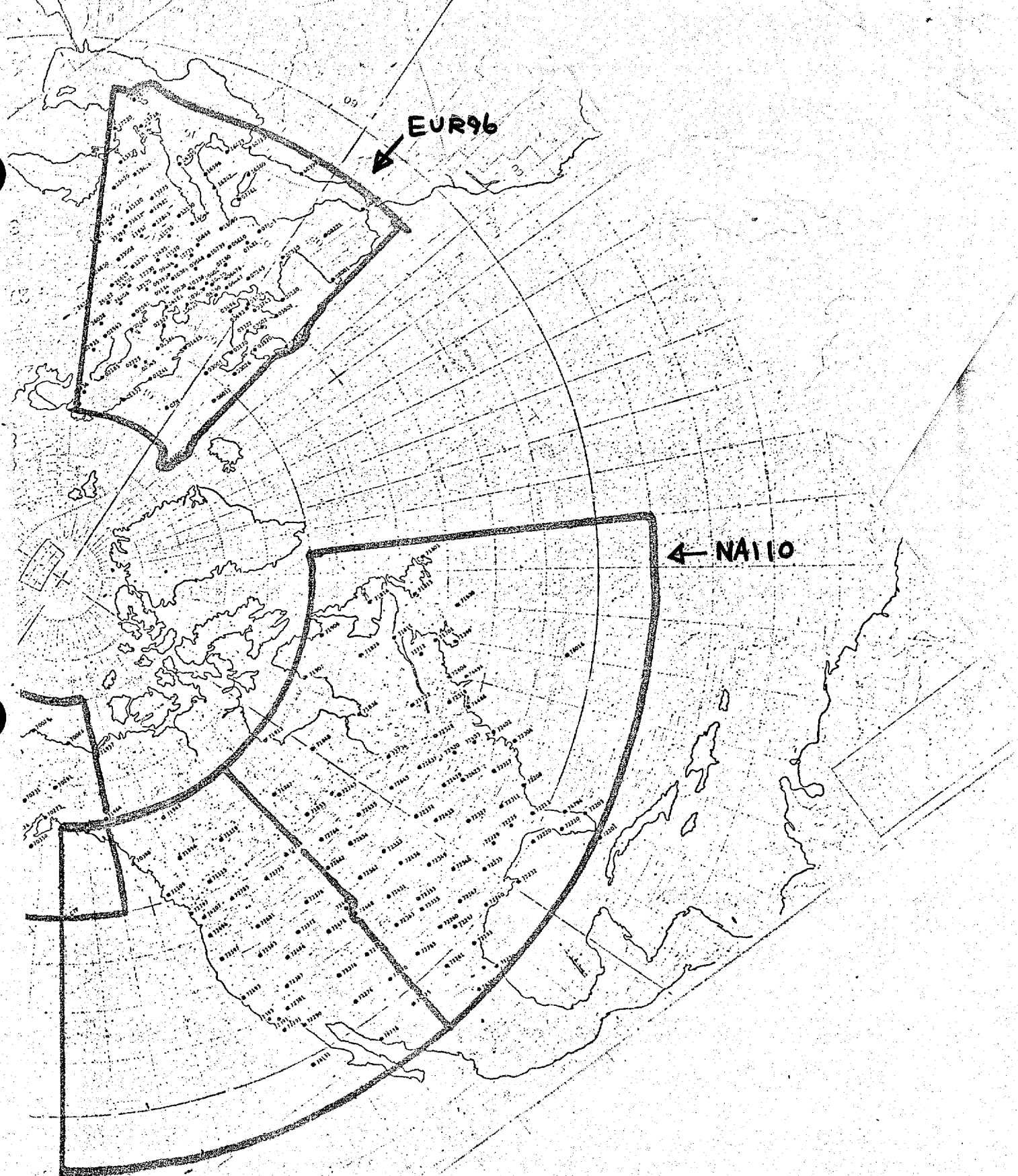


Figure 1. SUMAC verification areas NA110 and EUR96.

results of this test. Ideally one would want to choose cases in which cyclonic and anticyclonic curvature were distributed in equal amounts among troughs and ridges, respectively. Equation 4 implies that, for such cases in the northern hemisphere, the gradient wind exceeds the geostrophic wind in ridges to the north of the jet, and lags the geostrophic wind in troughs to the south of the jet (Figure 2). Graphs of gradient wind RMS error and bias were also plotted (Appendix B) for the 96 station EUR96 area (Figure 1). The upper air height gradients in this area during May were weak in contrast to those over NA110. The RMS vector wind deviation and the bias of the gradient winds were considerably lower over EUR96, and the rapid decrease in bias with increasing k , observed over NA110, is only weakly present.

In view of the tendency for the RMS vector wind deviation (gradient vs observed) to reach a minimum for $0.10 < k_1 < 0.25$, along with the large increase in negative bias for increasing values of k_1 , the value $k_1 = 0.15$ at all mandatory levels from 850 to 100 mb was chosen as the optimum value of k_1 . As a test, winds were computed from a 12Z 21 October 1979 Optimum Interpolation (O/I) height analysis. To verify that this change in k_1 improves the details of the wind fields, winds computed using the old values, $k_1 = 0.2, 0.2, 0.3, 0.3$ at 850, 500, 250, 100 mb, respectively, are shown in Figures 3 and 4, while winds computed using $k_1 = 0.15$ at each level are displayed in Figures 5 and 6. Observations are shown in Figure 7 and 8.

Comparing the gradient winds (Figures 3-6) with observations (Figures 7, 8) reveals that the gradient winds reproduce the overall details of the observed wind field quite well. Further comparison however, reveals that winds computed using $k_1 = 0.30$ (at 250 mb) were consistently weaker than those observed in troughs by from 20 to 110 percent, and stronger than observations in ridges by up to 40 percent. These characteristics are most marked in the trough-ridge-trough pattern extending from 45N, 145W into the western United States (Figure 3), in the broad trough over north central Europe (Figure 4). Notable differences between gradient winds and observations in the opposite sense occur in the ridge over the eastern U. S. (Figure 3), in the short-wave ridge near Iceland (Figure 4), where gradient winds are slightly weaker than observed, and in the trough over Tripoli (Figure 4), where gradient winds are stronger than observed. Gradient winds calculated using $k_1 = 0.15$ (Figures 5, 6) improve upon those calculated using $k = 0.30$ most notably in the trough-ridge-trough pattern west of 100W, in the trough north of Cuba (Figure 5), and in the trough along 30W, southeast of Greenland (Figure 6). Changing k_1 from 0.30 to 0.15 also reduces the winds in the ridges, but only 5 to 10 percent in most cases, and then only in sharp ridges. Large scale features, such as the broad trough over north central Europe (Figures 4, 6) remain unchanged by this change in k_1 .

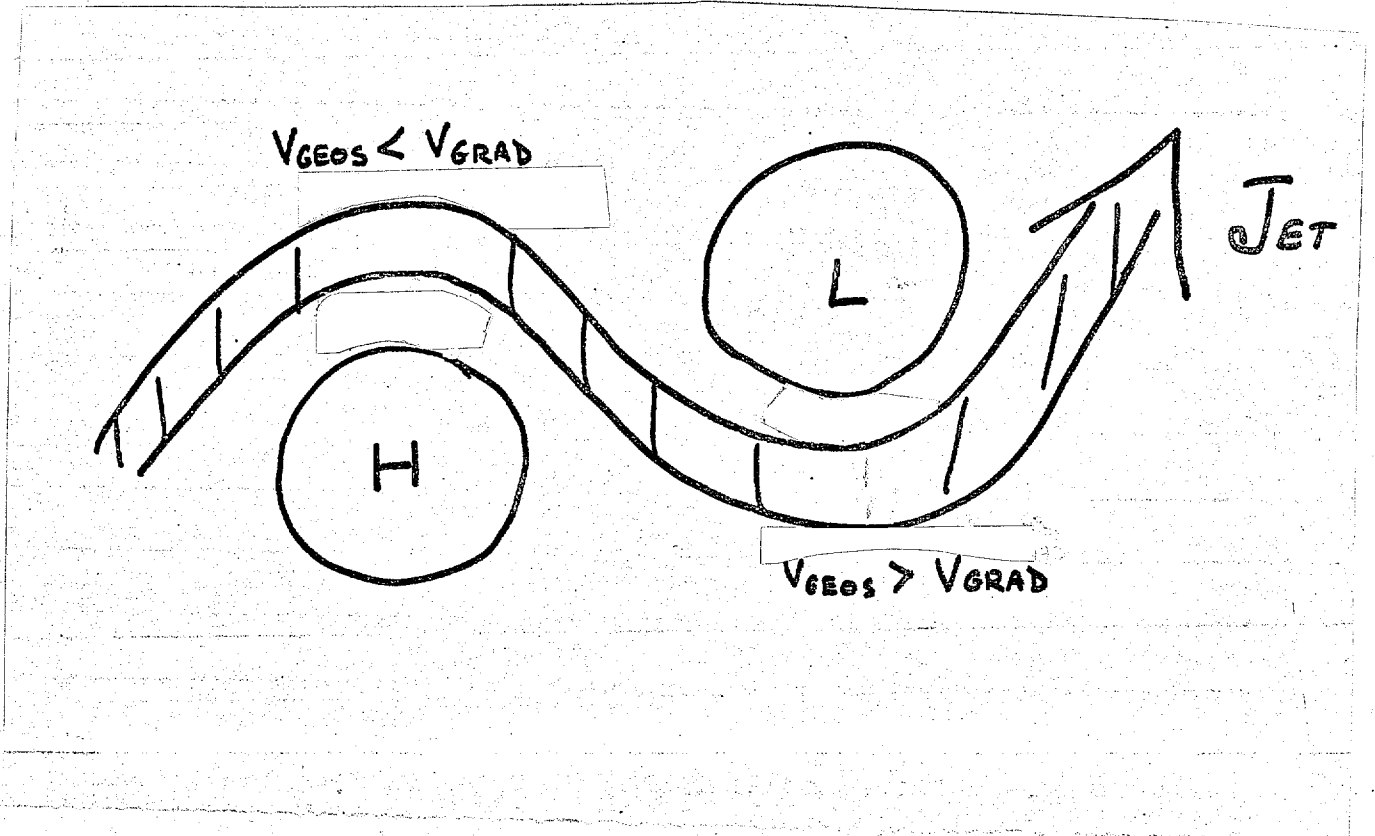


Figure 2. Physical interpretation of equation 4.

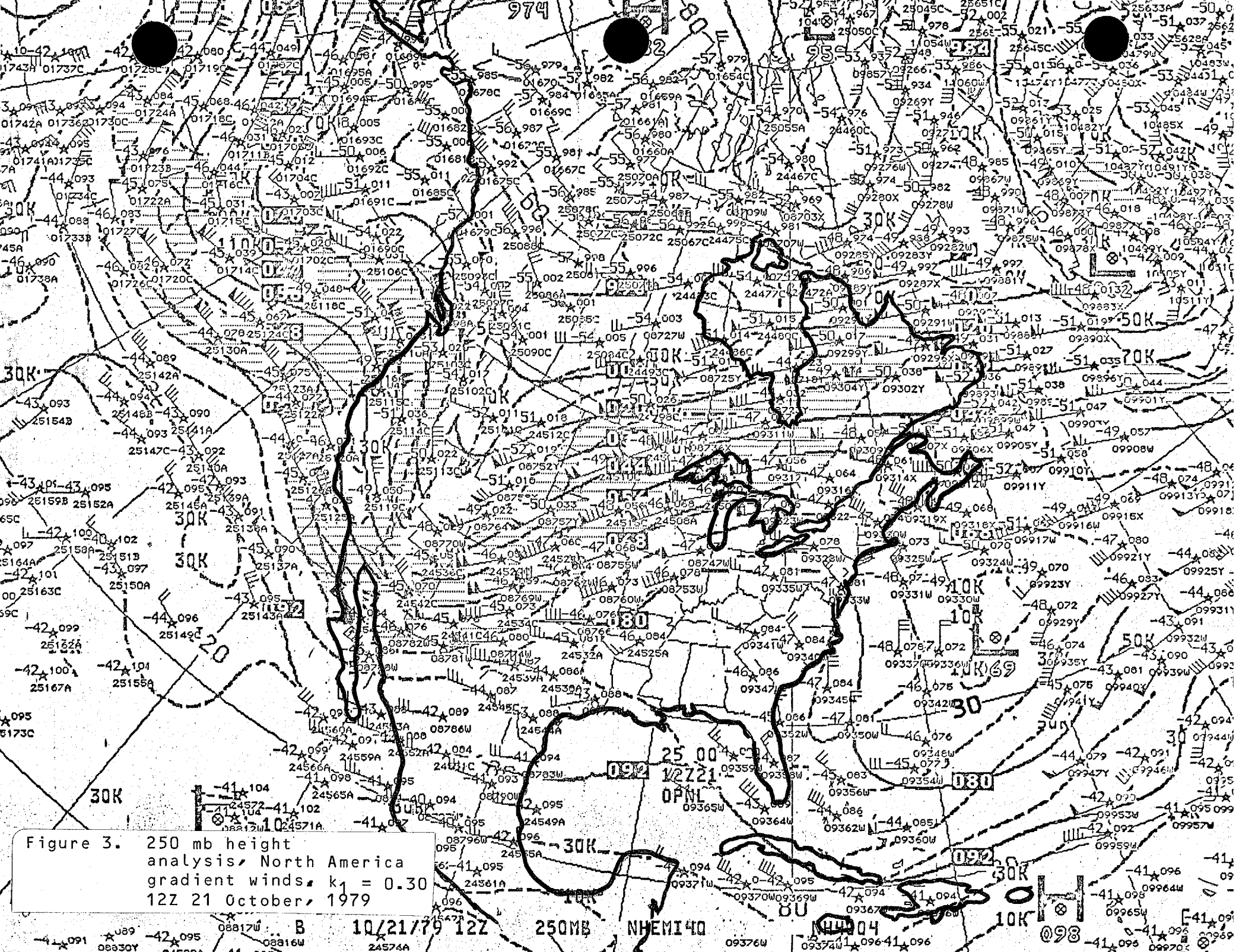


Figure 3. 250 mb height analysis, North America gradient winds, $k_1 = 0.30$ 12Z 21 October, 1979

10/21/79 12Z 250MB NHEMI40

08817W 08816W 24574A 09376W 09374W 09641*096 09376W 09374W 09641*096 09376W 09374W 09641*096

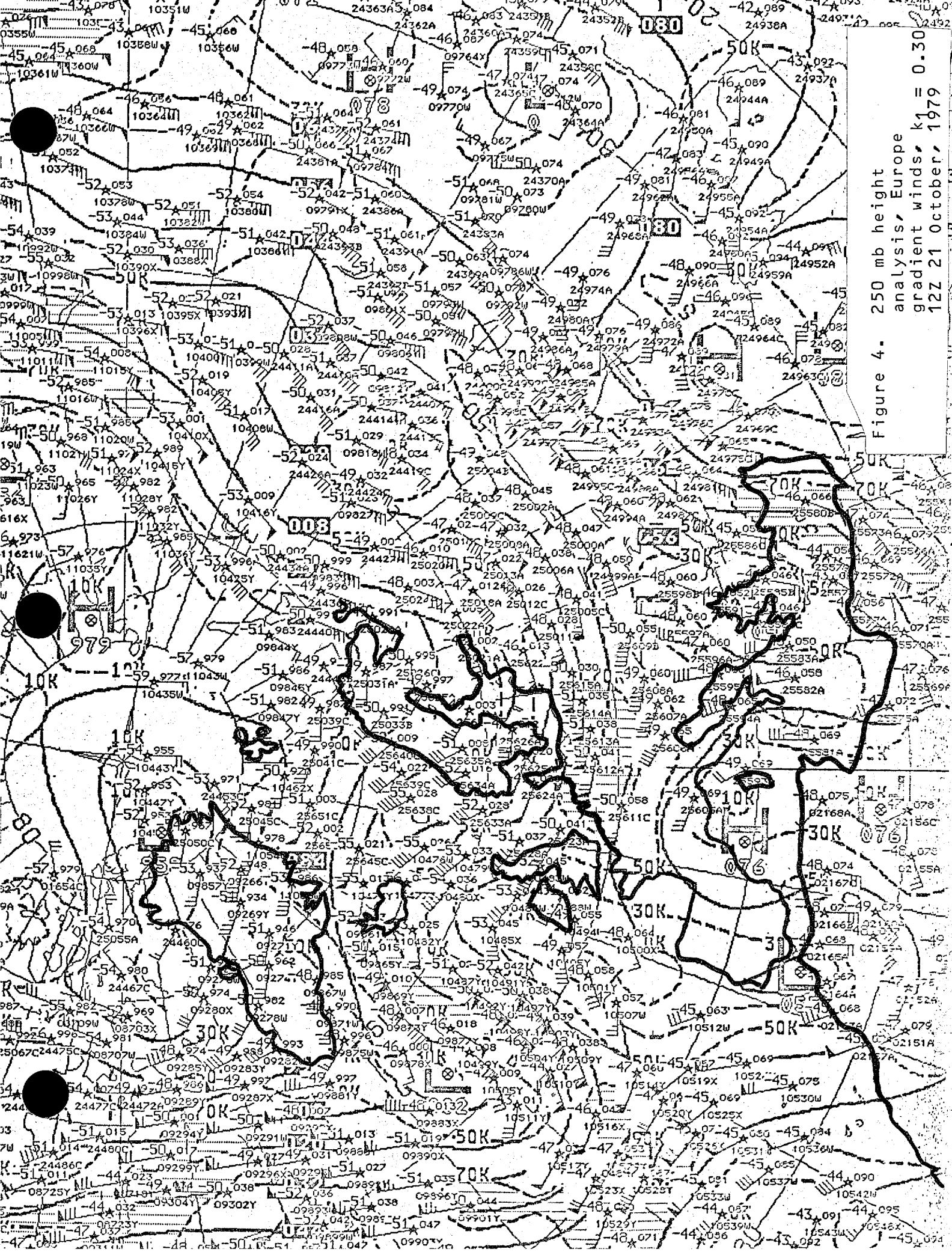


Figure 4. 250 mb height analysis, Europe gradient winds, $k_1 = 0.30$ 12Z 21 October, 1979

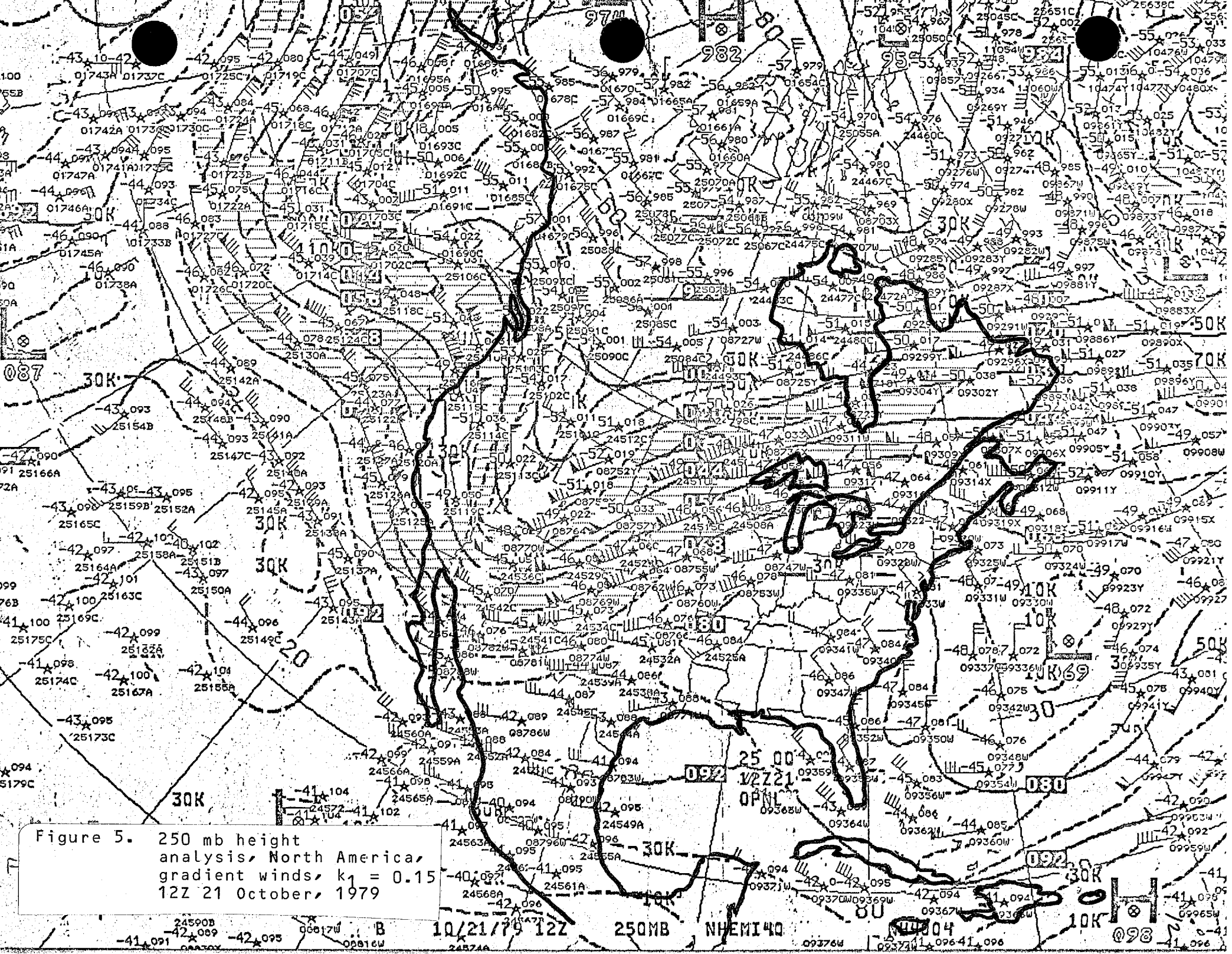


Figure 5. 250 mb height analysis, North America, gradient winds, $k_1 = 0.15$ 12Z 21 October, 1979

10/21/79 12Z 250MB NHEMI 40

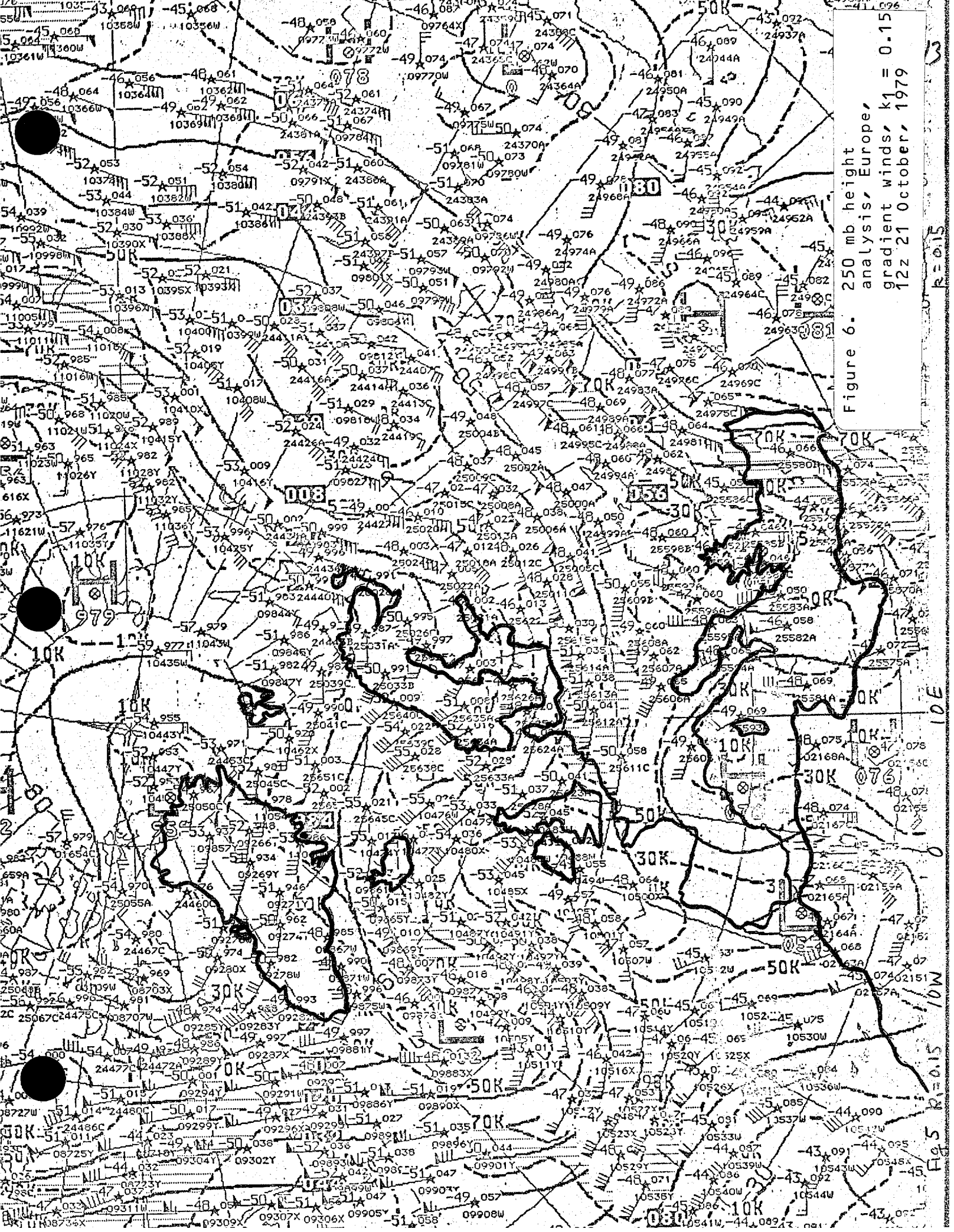


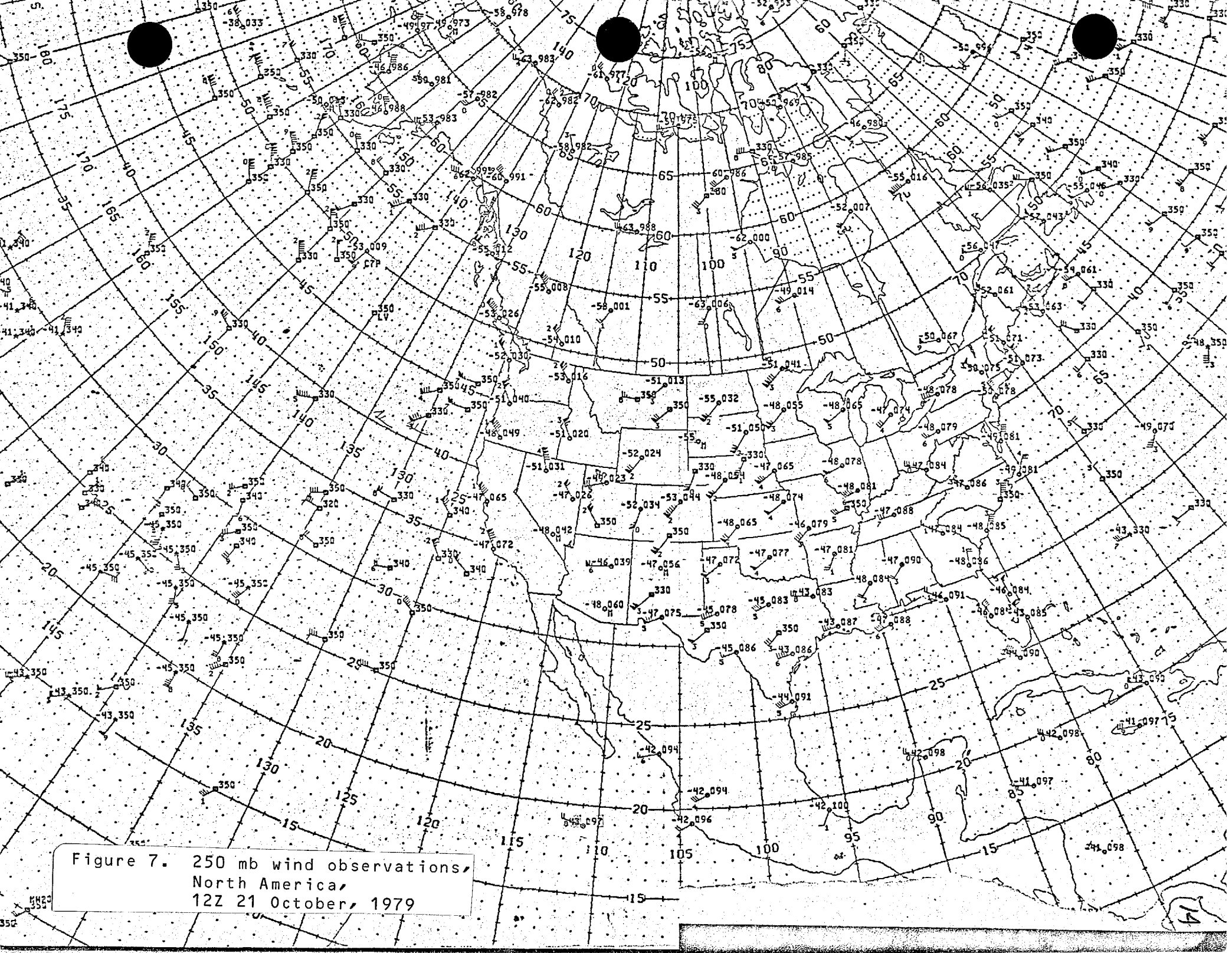
Figure 6. 250 mb height analysis, Europe, gradient winds, k1 = 0.15 12z 21 October, 1979

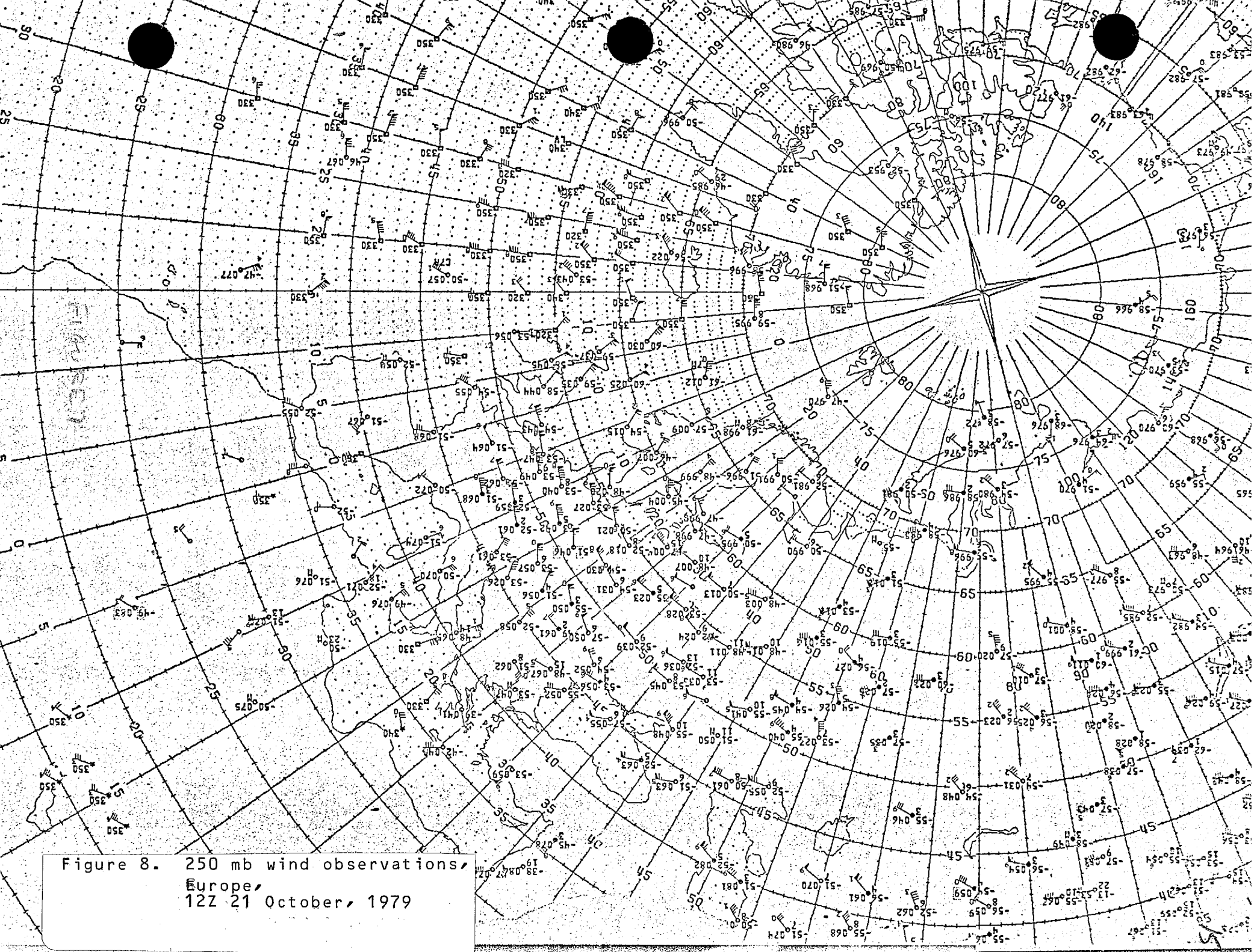
R=0.15

10E

10N

10S





Summary and Conclusions

A version of the gradient wind law currently in operational use at NMC has been studied in order to assess the usefulness of modifying one of its parameters, and its possible usefulness for providing winds to the O/I. A series of tests indicated that the RMS vector wind deviation (gradient vs. observed) for winds computed from this relation reached a minimum for values of the parameter k_1 of $0.1 < k_1 < 0.25$. The 250 mb mean speed error, or bias, was negative for all cases in both the NA110 and EUR96 areas. Further, this bias became increasingly negative with increasing k_1 , varying from about -1.0 ms^{-1} for $k_1 = 0.05$, to -3.0 ms^{-1} for $k_1 = 0.33$. Considering these RMS and bias variations, it was decided that a value of $k_1 = 0.15$, instead of the value $k_1 = 0.30$, currently used at 250 mb in the LFM, might result in improved gradient winds, especially with respect to their mean speed bias. Comparisons of winds calculated using both values of k_1 with each other, and with observations, confirmed that winds calculated using the updated k_1 brought wind speeds in most troughs into better agreement with observations, with only slight decreases in wind speeds in ridges. This certainly can be regarded as an improvement, at least for the 12Z 21 Oct 79 case. Table 1 lists the value of k_1 currently used in the LFM and gives a suggested list of updated values for all standard levels based on the results of this study.

Table 1. Current and Suggested Values of Parameter k_1 in LFM

<u>Pressure level (mb)</u>	<u>Current Value</u>	<u>Suggested Value</u>
1000	0.0	0.0
850	0.1	0.1
700	0.2	0.1
500	0.2	0.15
400	0.2	0.15
300	0.2	0.15
250	0.3	0.15
200	0.3	0.15
150	0.3	0.15
100	0.3	0.1
70	0.3	0.1
50	0.3	0.1

References

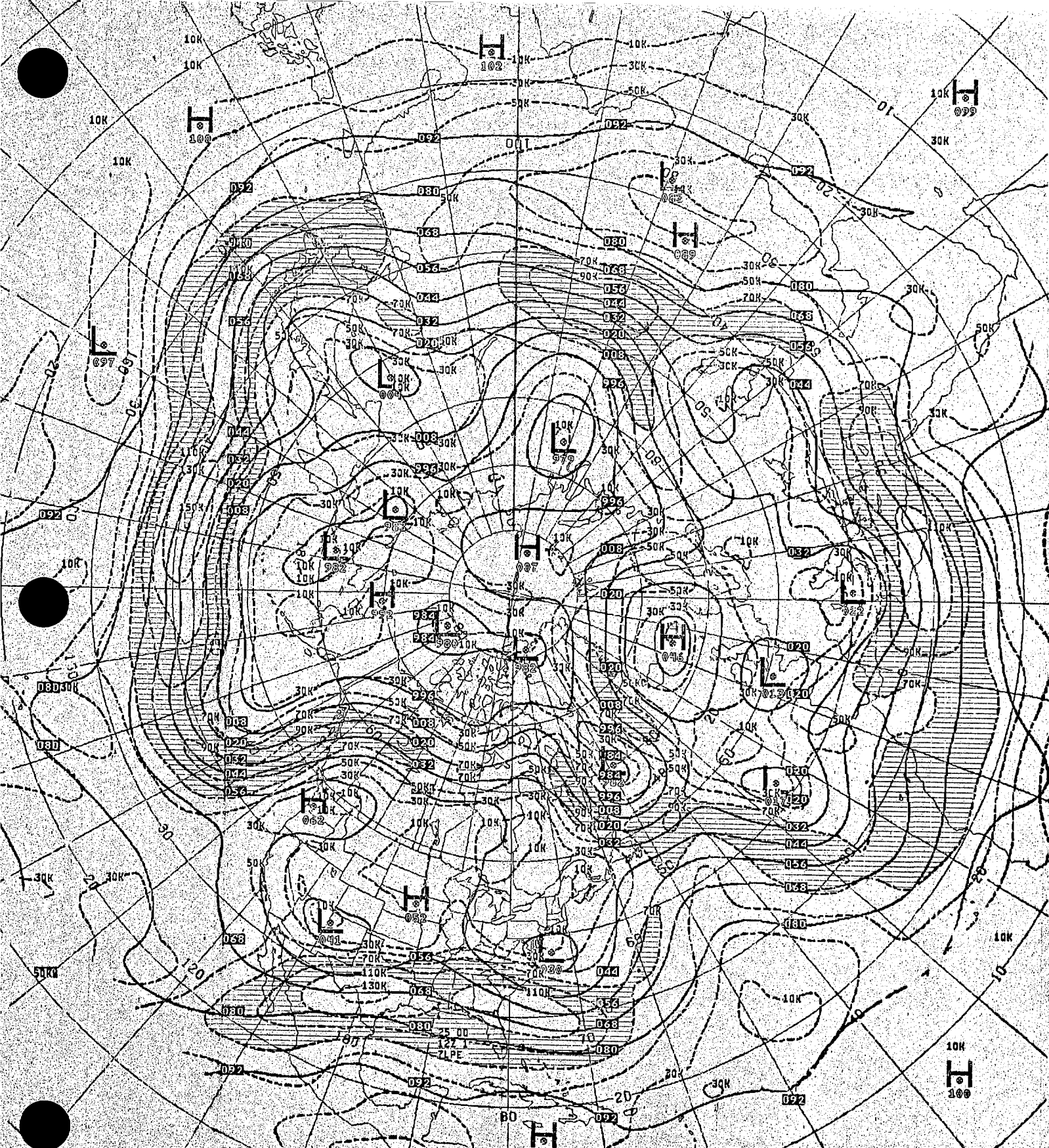
Brown, John, A., 1971: New Initialization Procedure for the 6-Layer (PE) Numerical Prediction Model. Technical Procedures Bulletin No. 65, August 1971.

Acknowledgements

I wish to express appreciation to A. J. Desmarais for providing both a coded version of the gradient wind equation, and the impetus to carry out this study. Conversations with Dr. John A. Brown clarified many questions. John R. Ward supplied the height-analysis for the 12Z 21 October 1979 case.

APPENDIX A

250 mb Height-Isotach Analyses

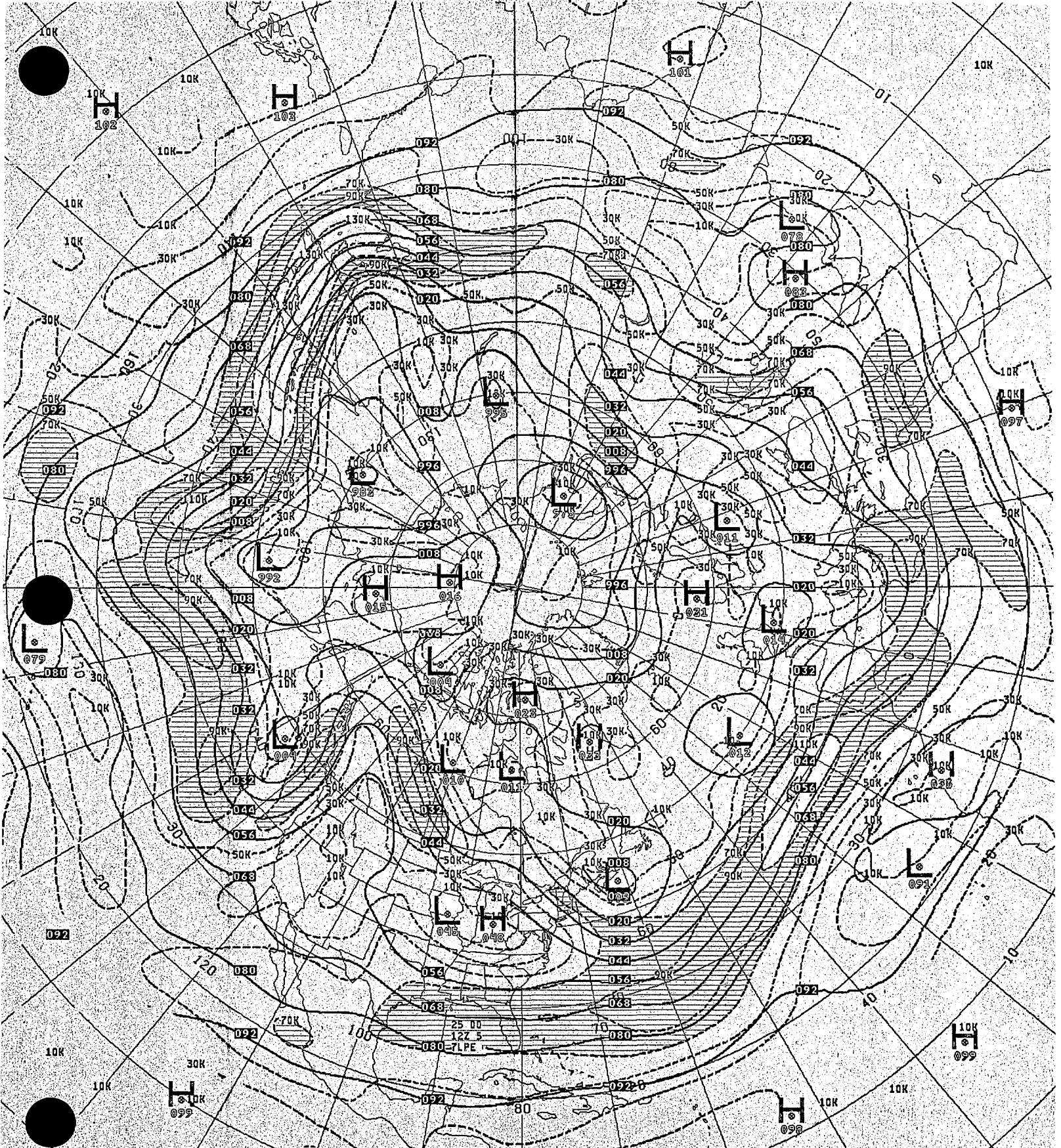


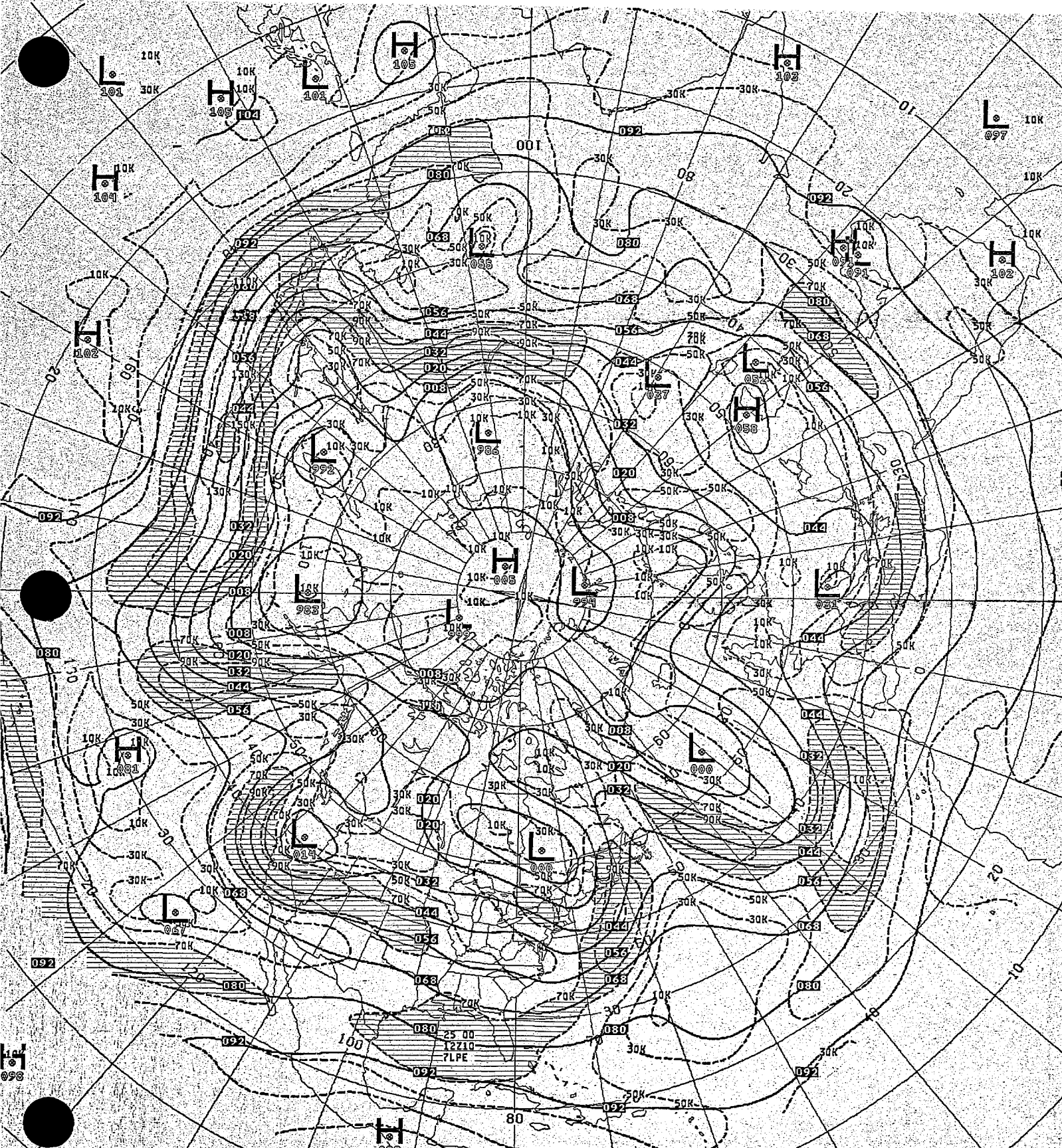
V419

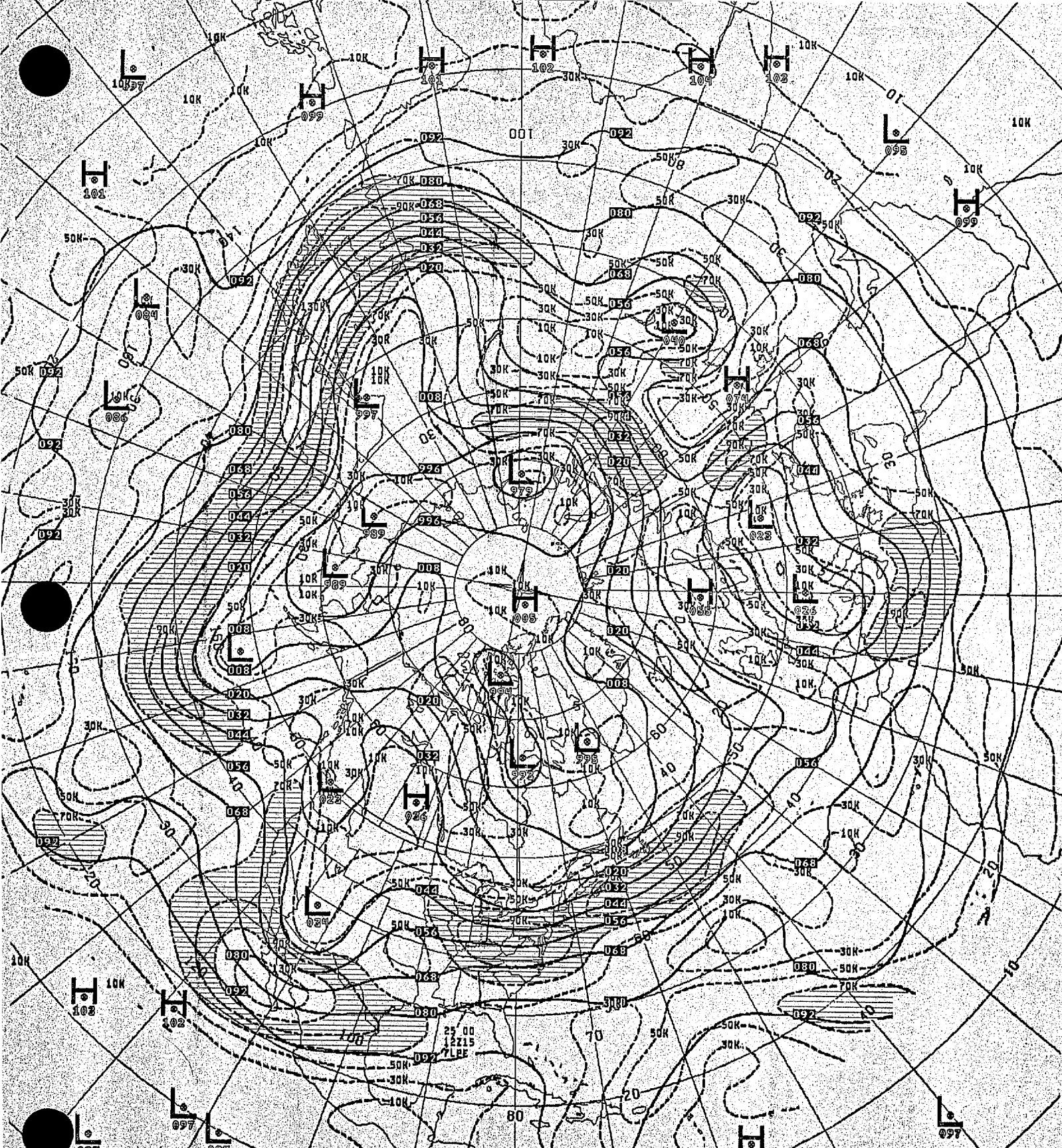
250MB ANALYSIS

HEIGHTS/ISOTACHS

12Z THU 1 MAY 1980 J624





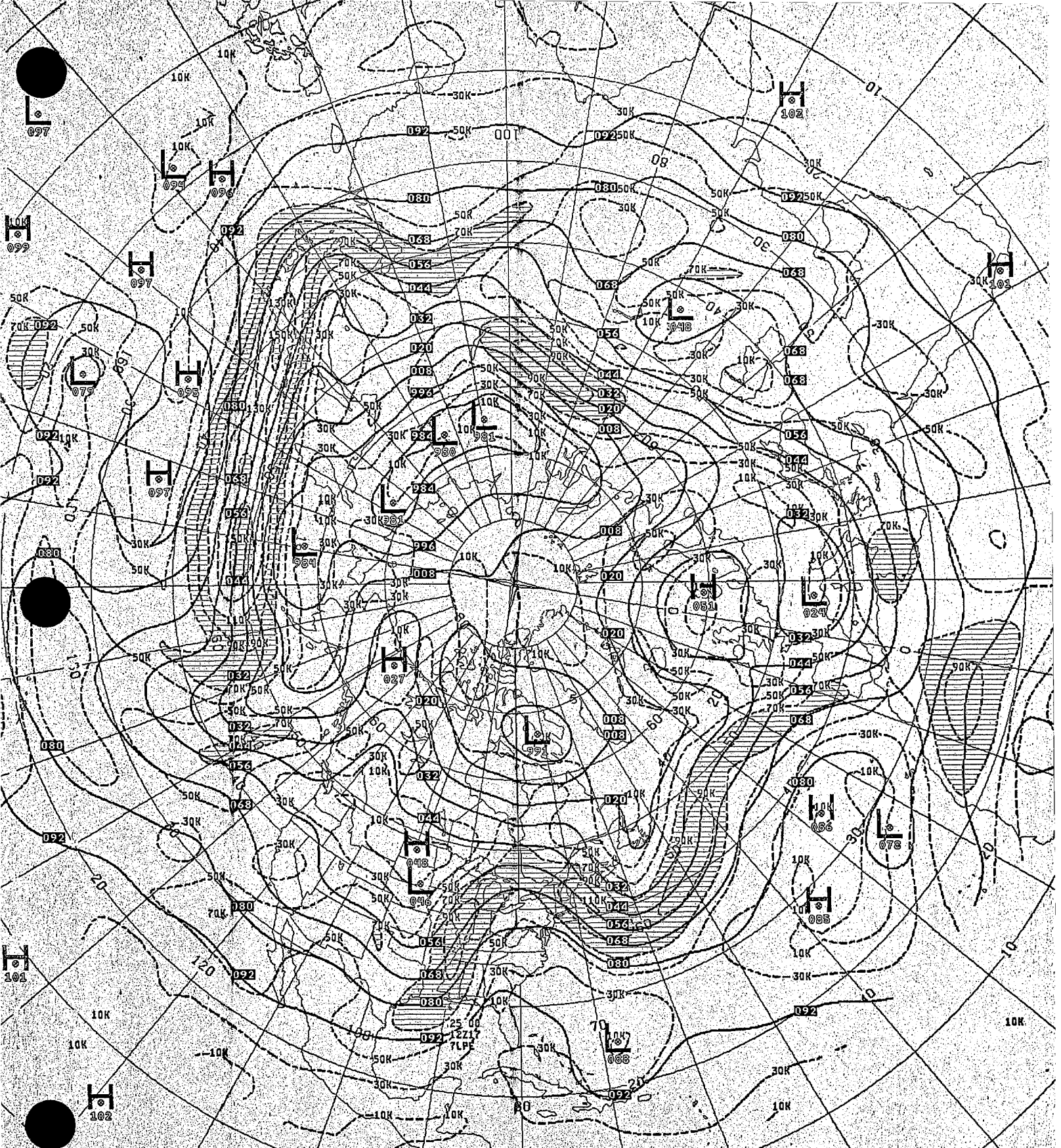


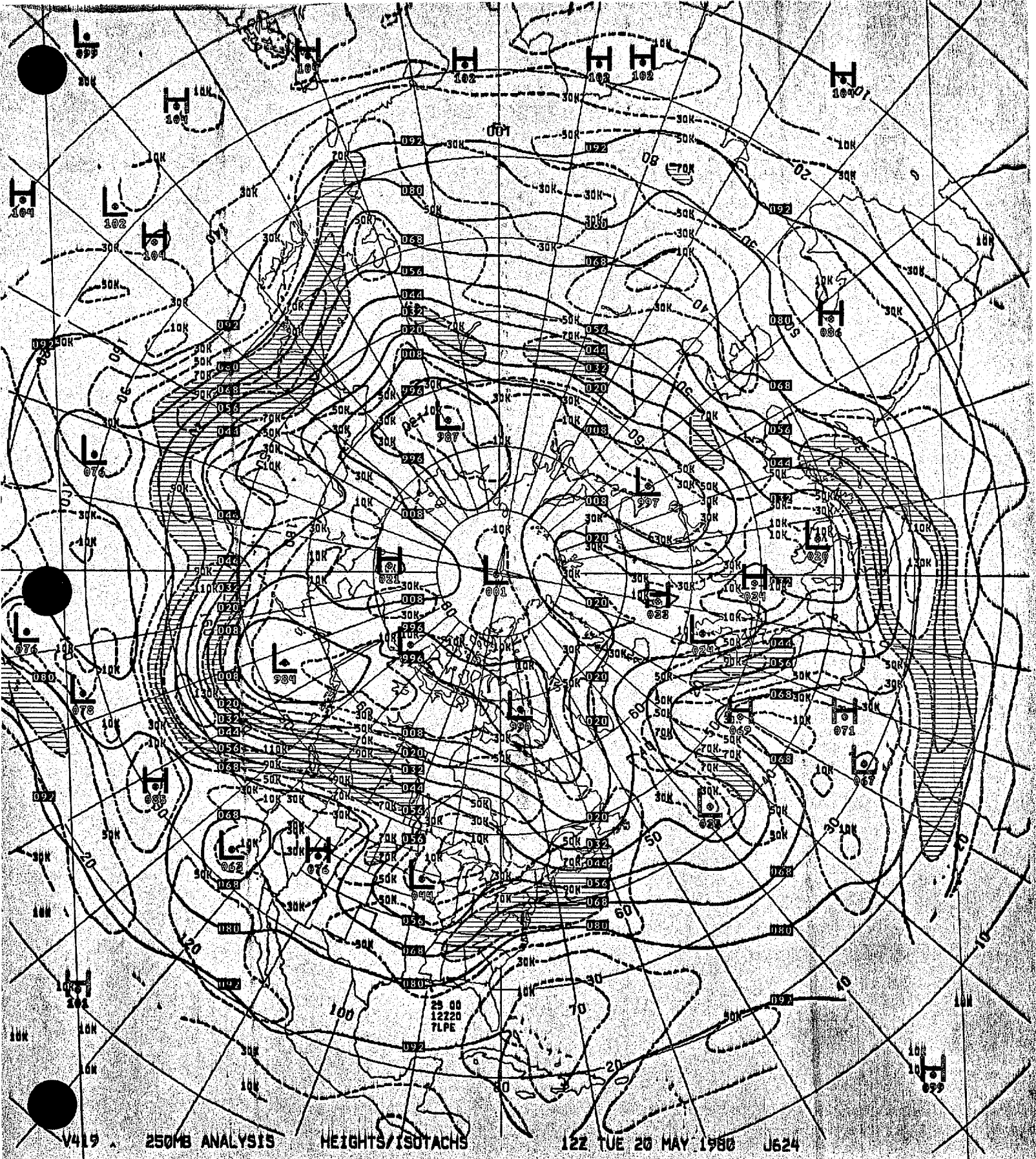
V419 250MB ANALYSIS

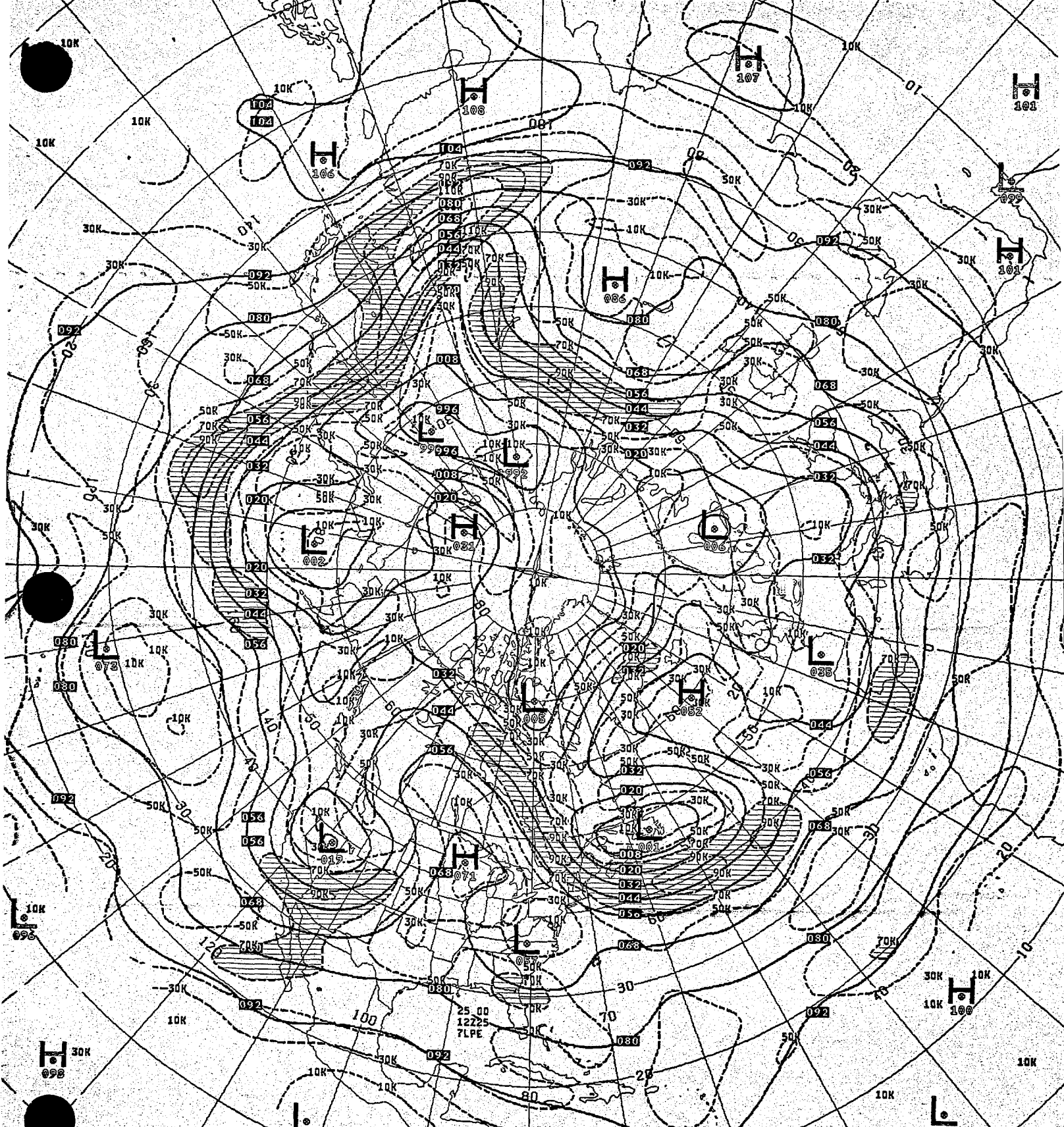
HEIGHTS/ISOTACHS

12Z THU 15 MAY 1980

J624







V419

250MB ANALYSIS

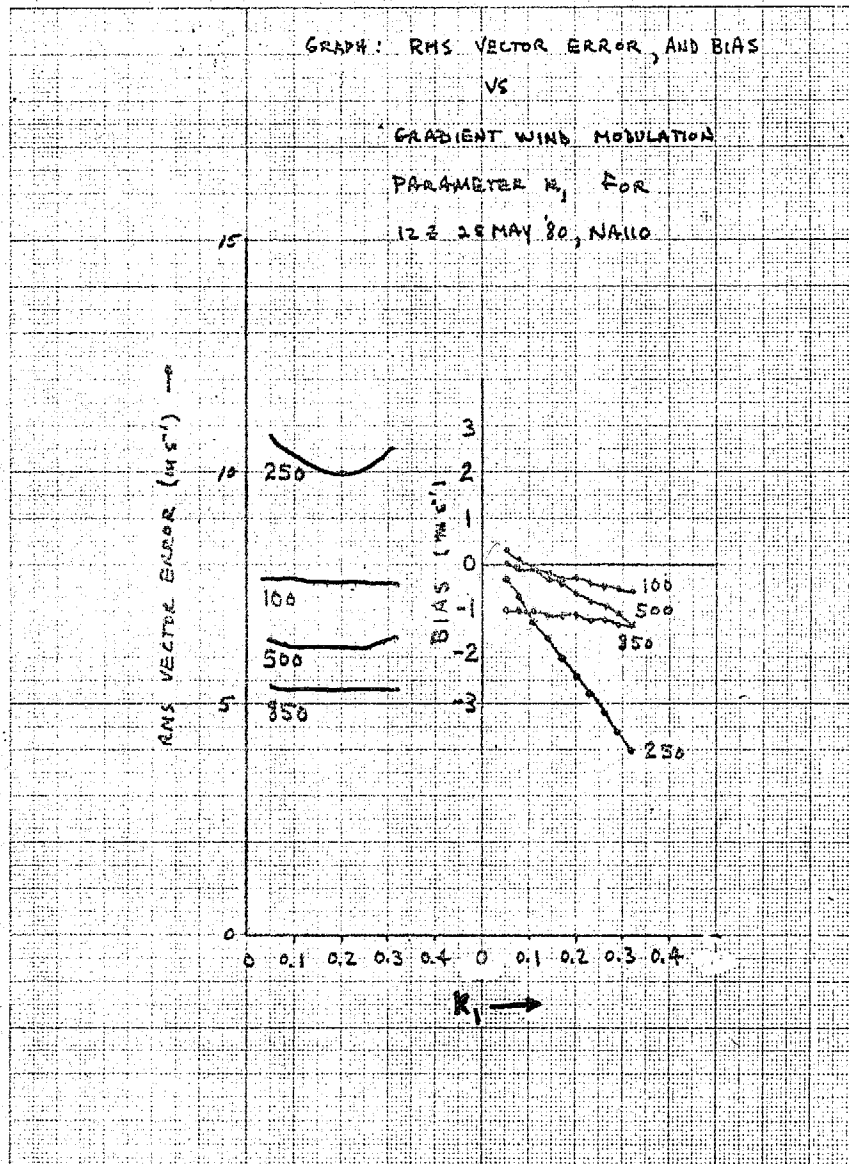
HEIGHTS/ISOTACHS

12Z SUN 25 MAY 1980

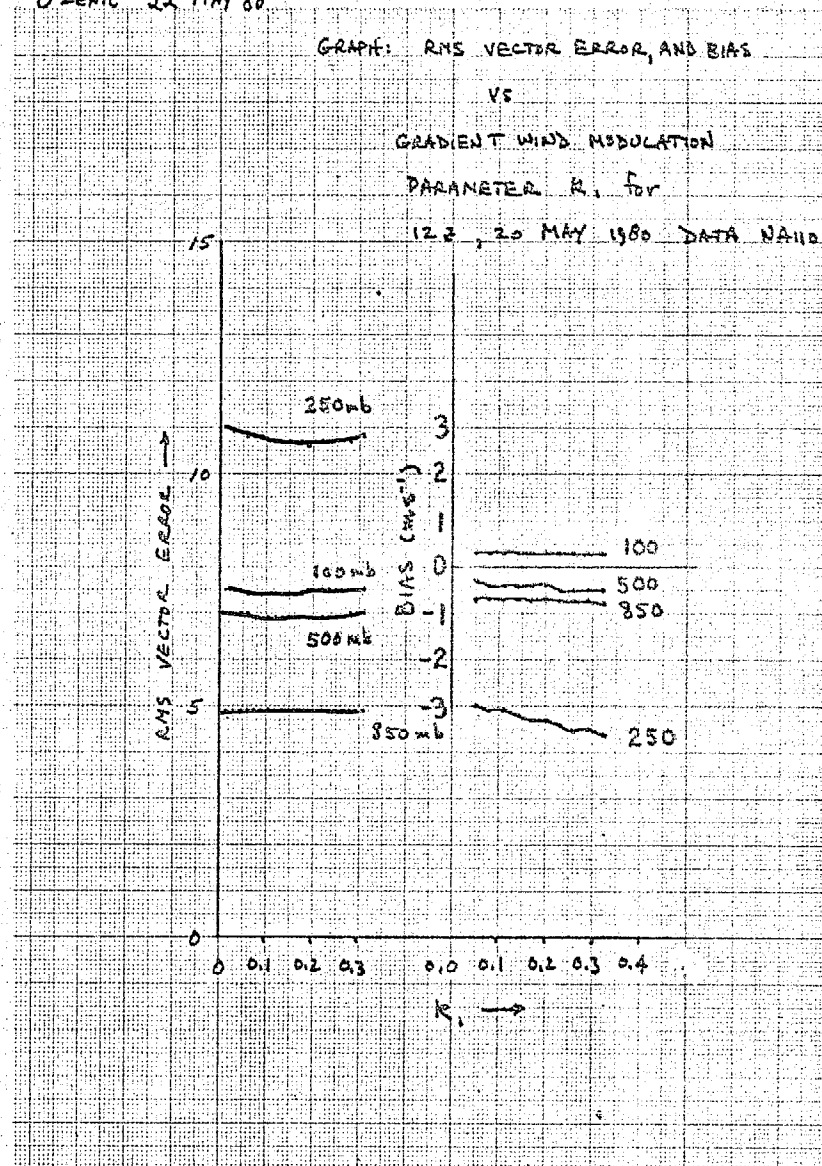
J624

APPENDIX B

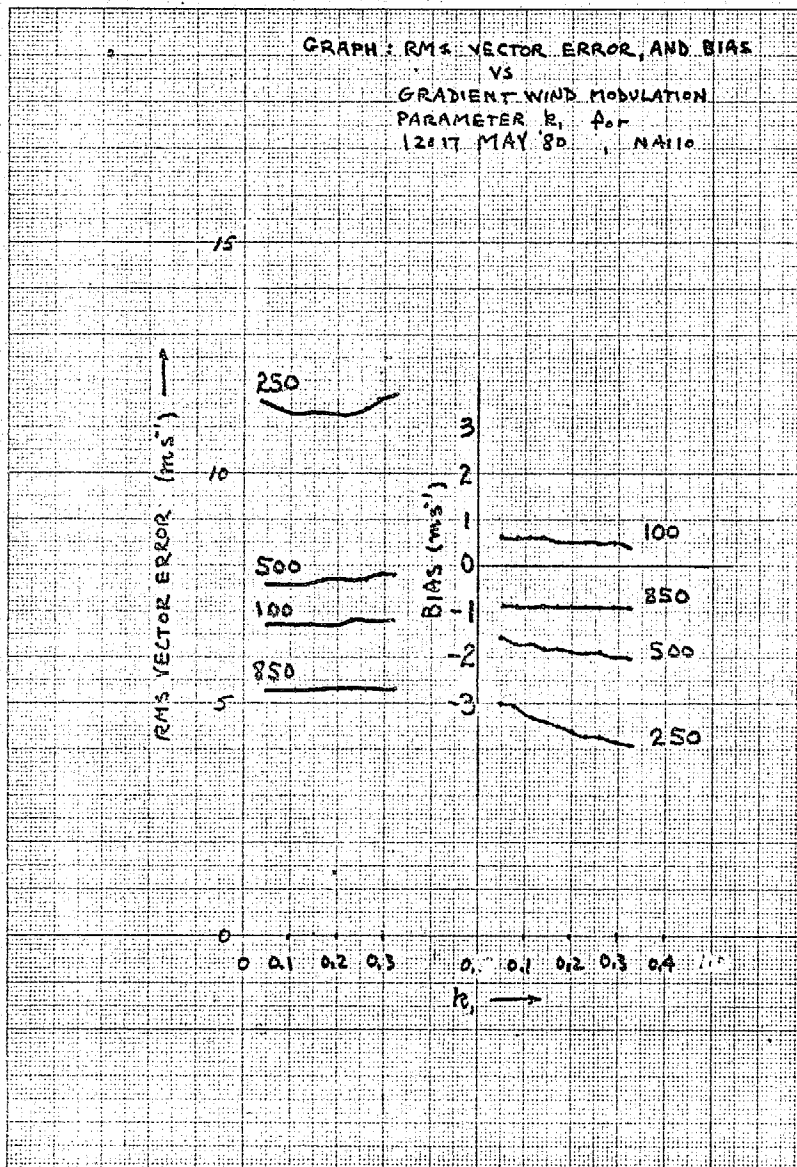
RMS vector wind deviation and bias from SUMAC verifications
(gradient winds vs. observed winds)



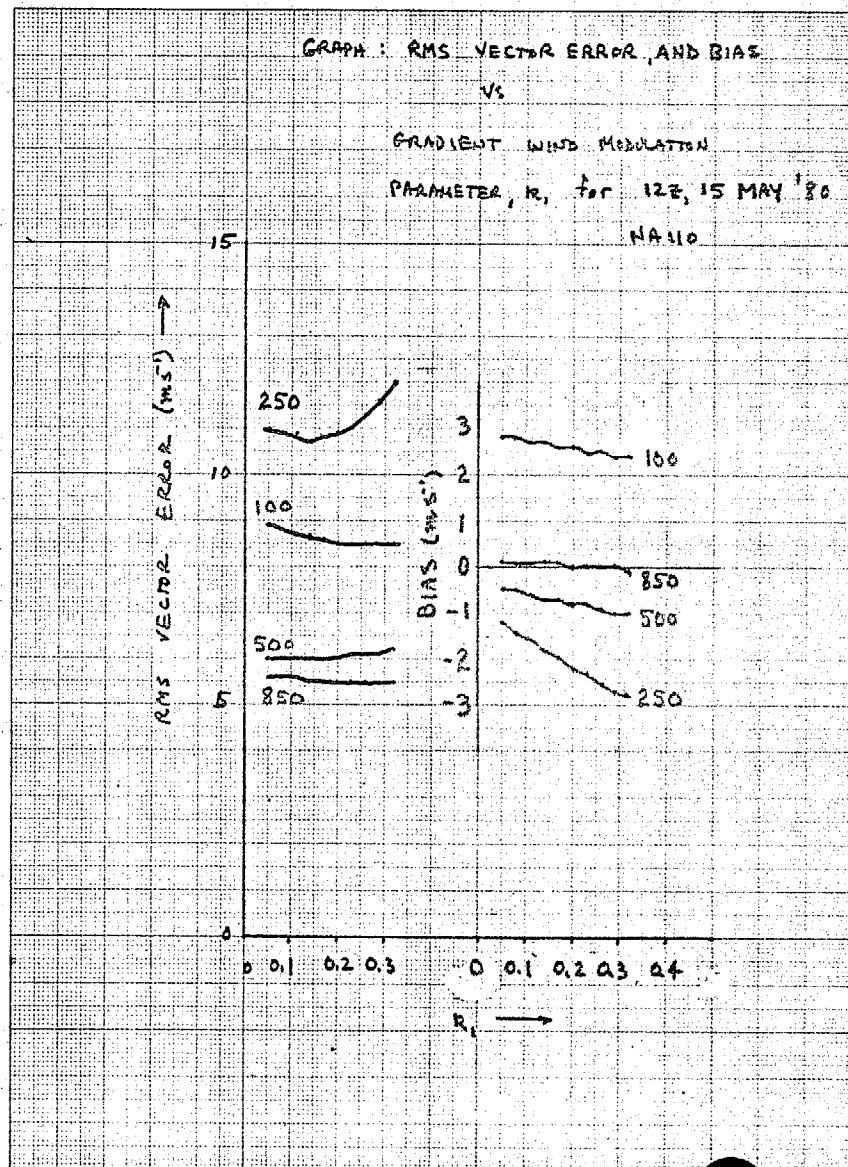
O'LENIC 22 MAY 80



GRAPH: RMS VECTOR ERROR, AND BIAS
VS
GRADIENT WIND MODULATION
PARAMETER R_1 for
12:17 MAY '80, NA110.



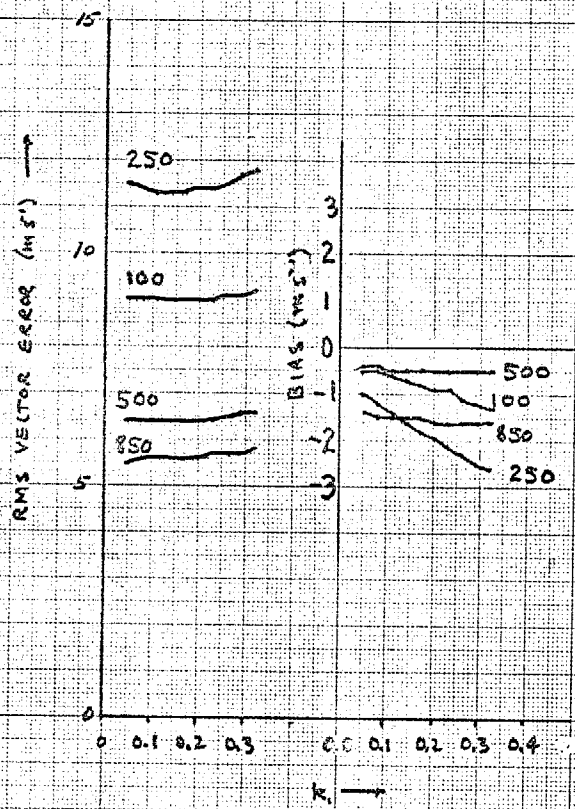
GRAPH: RMS VECTOR ERROR, AND BIAS
VS
GRADIENT WIND MODULATION
PARAMETER, R_1 for 12:15 MAY '80
NA110



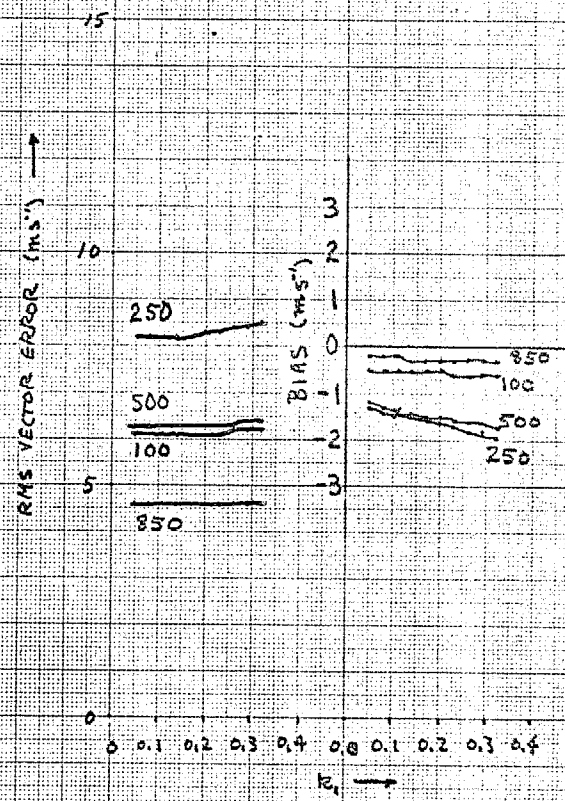
DIRTYZEN CORPORATION
MADE IN U.S.A.

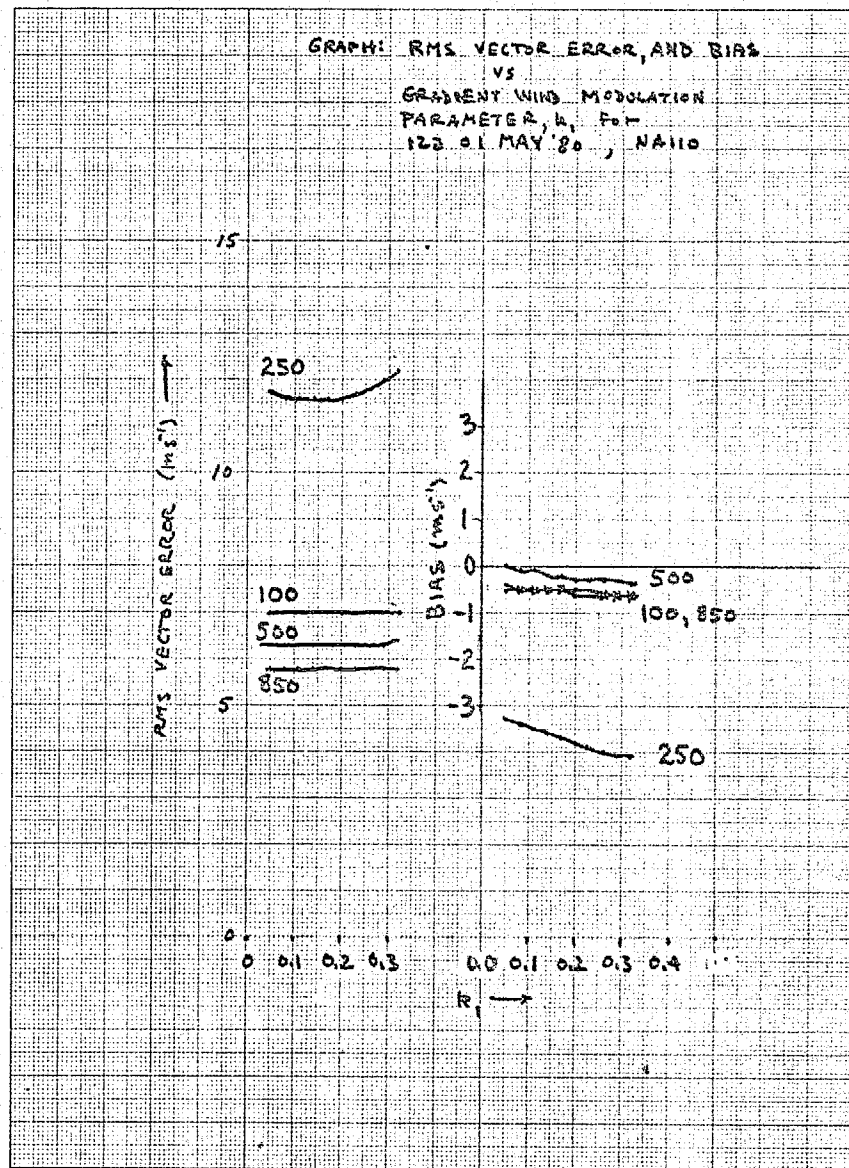
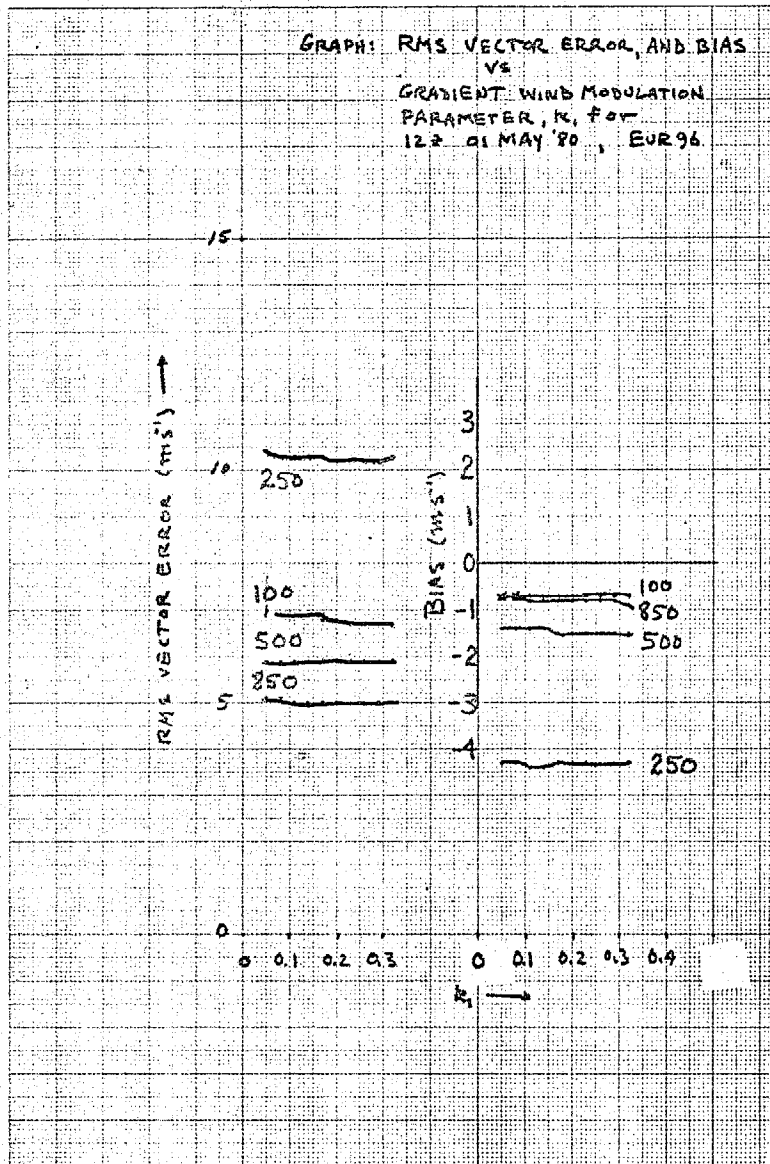
NO. 340-A DIRTYZEN GRAPH PAPER
MILWAUKEE

GRAPH: RMS VECTOR ERROR, AND BIAS
VS
GRADIENT WIND MODULATION
PARAMETER M_1 FOR
12Z 10 MAY '80, NALLO

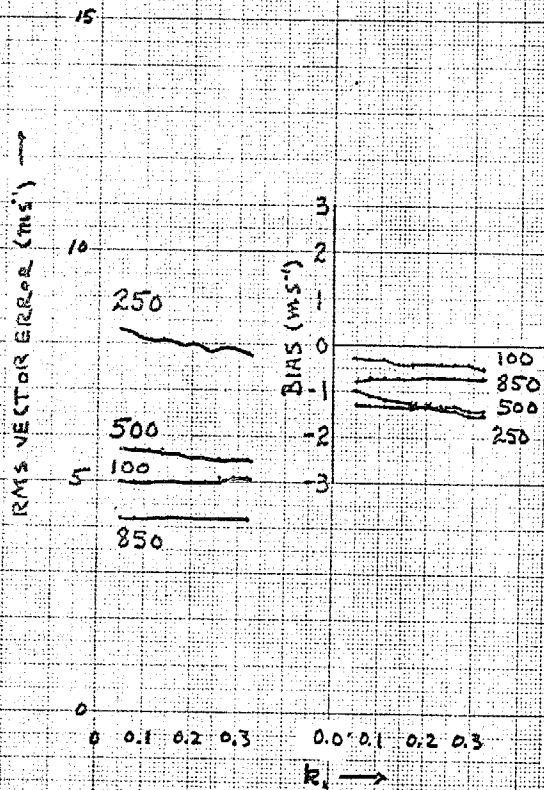


GRAPH: RMS VECTOR ERROR, AND BIAS
VS
GRADIENT WIND MODULATION
PARAMETER R_1 FOR
12Z 05 MAY '80, NALLO

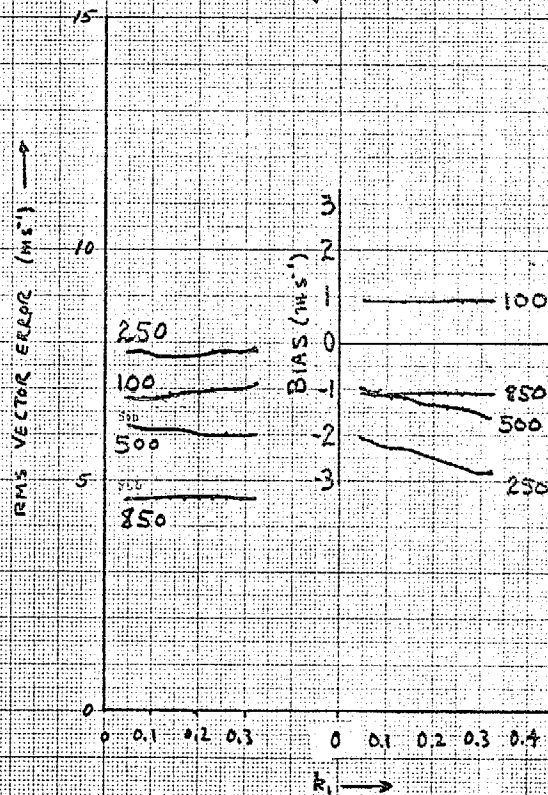


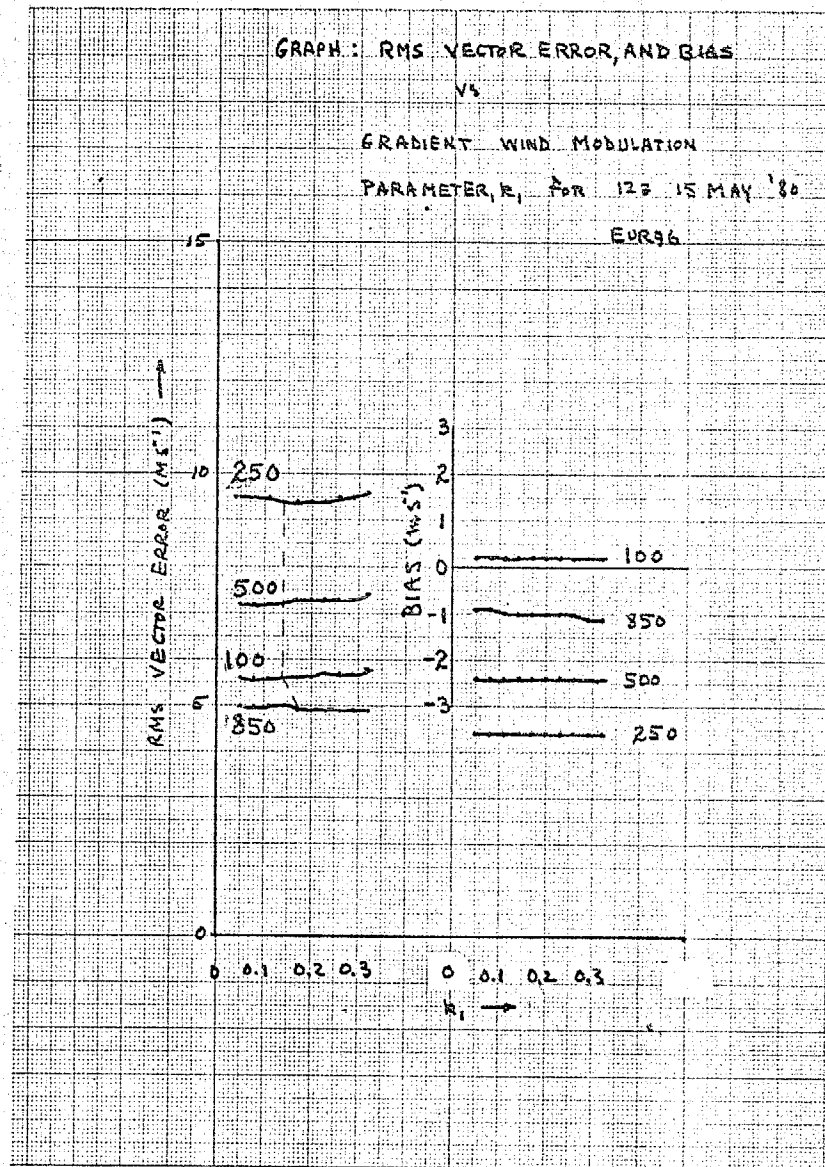
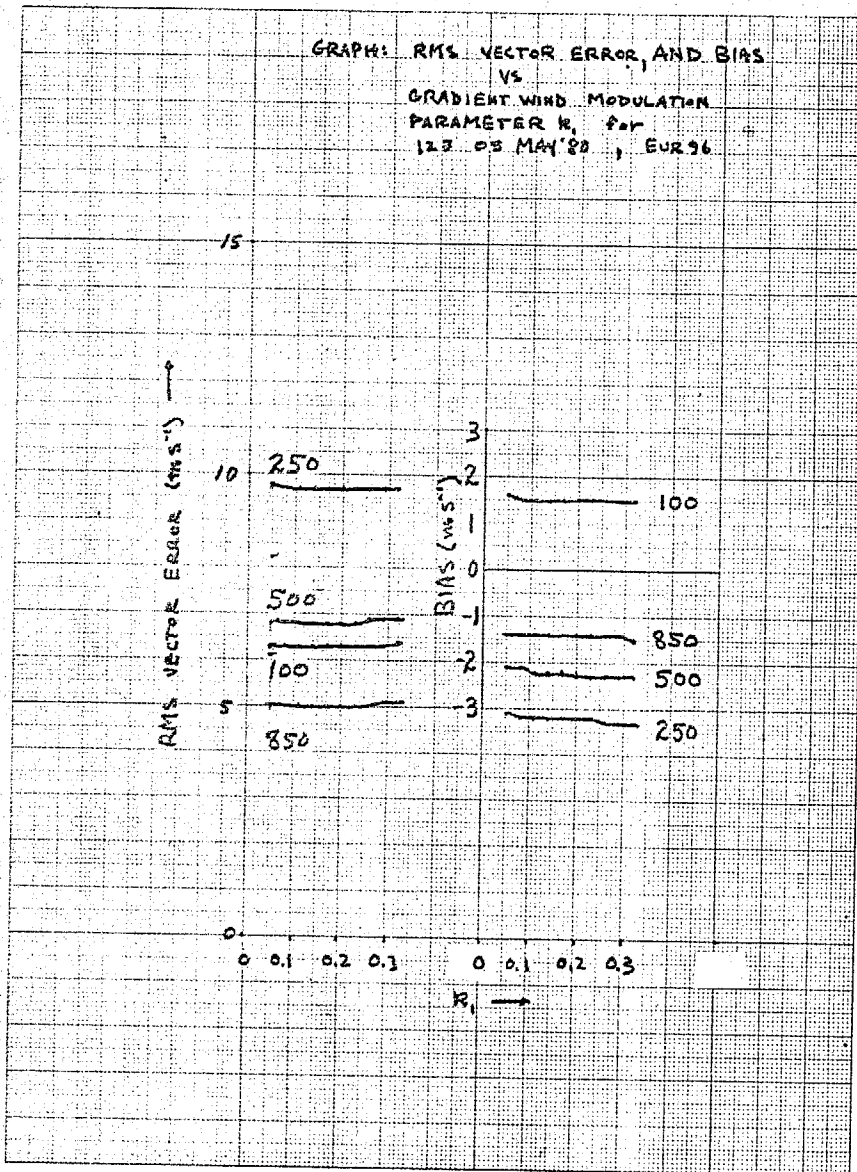


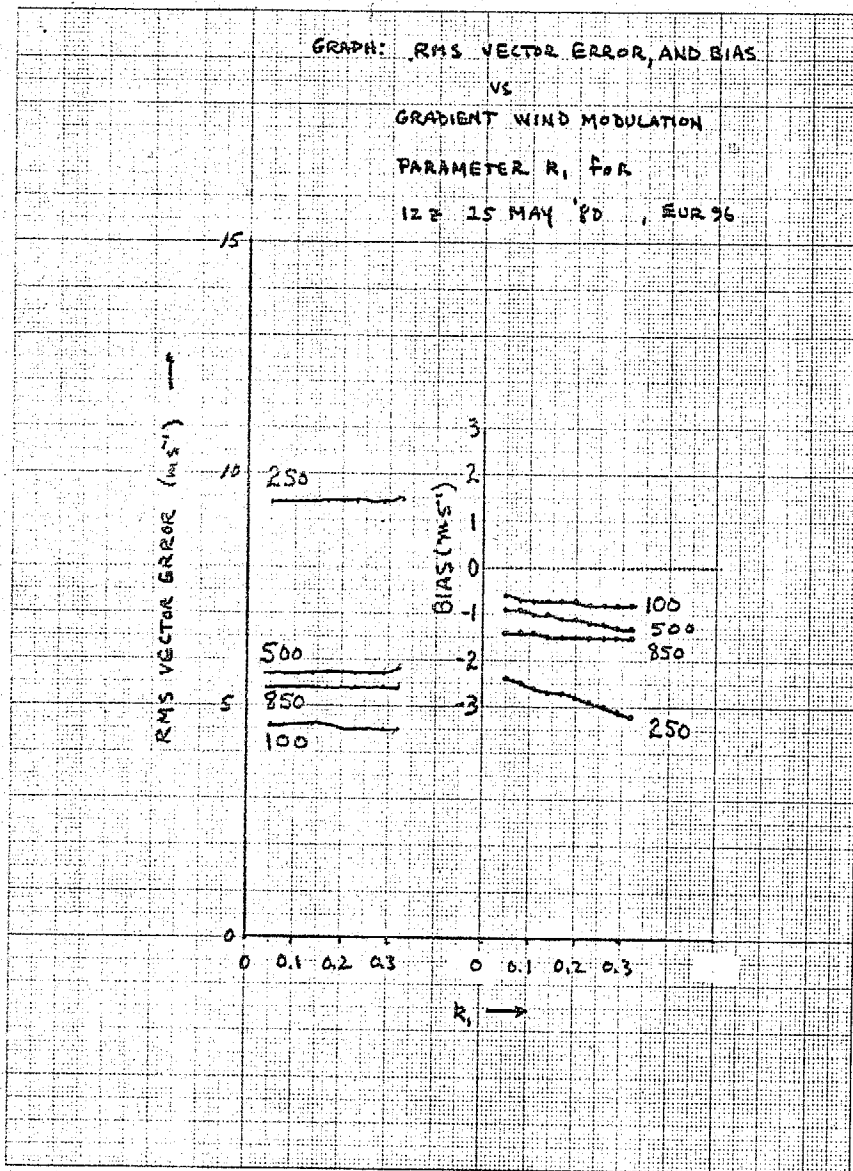
GRAPH: RMS VECTOR ERROR, AND BIAS
vs
GRADIENT WIND MODULATION
PARAMETER k_1 for
123 17 MAY '80, EUR96



GRAPH: RMS VECTOR ERROR, AND BIAS
vs
GRADIENT WIND MODULATION
PARAMETER k_1 for
123 10 MAY '80, EUR96







LENIC 22 MAY

